

Laboratory Testing of Paving Mixes – Dynamic Material Functions and Wheel Tracking Tests

J. Zak¹⁺, J. Stastna², L. Zanzotto², and D. MacLeod³

Abstract: Five asphalt paving mixes prepared with different asphalt binders (one conventional, two oxidized, and two modified by styrene-butadiene-styrene copolymer, 2% and 4% by weight) were studied in small amplitude oscillation and wheel tracking tests. The main focus of the study was to investigate these materials at a relatively high service temperature (58°C). From dynamic testing at temperatures ranging from -10°C to 80°C, the master curves of dynamic material functions (storage modulus, loss modulus, and loss tangent) were prepared at a reference temperature of 58°C. The relaxation and retardation spectra were calculated for all the materials, and the corresponding (compressive) compliance, $D(t)$ (linear viscoelastic), was also determined from the retardation spectrum. It was shown that $D(t)$ can be effectively approximated from the magnitude of the complex compliance by transforming the domain of the reduced frequencies to the time domain. From the wheel tracking test performed at 58°C, the accumulated compliance function (deformations larger than in the dynamic tests) was calculated and appended to the linear viscoelastic $D(t)$. A simple model of the compounded compliance with stretched time (developed earlier) was used. It was shown that, in most of the tested materials, the information from the dynamic testing seemed to be poorly correlated with the trend of the compliance obtained from the wheel tracking data when the compounded compliance was plotted. On the other hand, when the model of compliance was fitted only to a subset of the linear viscoelastic data (the subset generated by points defining the peak of the loss tensile modulus), the accumulated compliance from the wheel tracking test can be estimated by the same model.

DOI:10.6135/ijprt.org.tw/2013.6(3).147

Key words: Compliance function; Dynamic testing; Paving mix; Wheel tracking.

Introduction

Asphalt paving mix is a frequently used construction material. It may not be the most sophisticated material; however, it is widely produced worldwide. The investment in transportation infrastructure (a great part of which is built with asphalt paving mix) represents a big portion of the gross domestic product (GDP) of countries around the world.

With increasing volume and traffic loads, the demand for better performing asphalt paving materials is high. These materials are basically composed of irregular aggregates with a small amount of asphalt binder and a low volume fraction of air voids. Although asphalt forms only a small part of asphalt paving mix, it determines the viscoelastic properties of these materials. Quite often, the asphalt binder is modified either chemically or by blending it with various polymeric modifiers [1-10]. The use of polymer modified asphalt is steadily increasing, because it leads to the production of paving materials with less low-temperature cracking, less rutting, and improved fatigue cracking resistance [11].

Asphalt paving mix is a multiphase system with many components, some of which have complicated internal structures with high-temperature susceptibility (conventional or polymer modified asphalt binder). Notwithstanding its complicated structure, the thermo-mechanical behavior of asphalt paving mix can be modeled with the help of the theory of viscoelasticity [12-14].

The properties of asphalt paving mixes at high service temperatures are studied in this research. At such temperatures, the most serious distress mode is the rutting phenomenon observed in many asphalt paved roads [15, 16]. Rutting can be characterized as an irreversible deformation due to the flow of asphalt binder accompanied by the displacement of aggregate matrix and decrease in the air content [16-18]. When the material is subjected to a compressive and shear stresses of sufficiently high amplitudes, it attains a state of irreversible deformation and finally ruptures.

These changes in the materials are associated with structural inhomogeneities on various levels [19]. The formation of inhomogeneities in viscoelastic materials at temperatures above the glass transition temperature can be influenced by the presence of filler particles, viscoelastic relaxation, formation of a crystalline phase, and the history of repetitive stressing. Repetitive stress is frequently used as the primary testing method, when the strength and durability of a material is the main engineering concern. Although large deformations certainly occur in these tests (material exhibits nonlinear behavior), the linear viscoelastic properties of the studied materials have an important impact on its behavior in the nonlinear viscoelastic domain. Certainly, from the two tests considered here, one cannot claim a complete knowledge of all processes appearing during the transition from linear to nonlinear behavior of the studied material. The aim of this research was to

¹ Department of Road Structures, Faculty of Civil Engineering, Czech Technical University, Prague, Thakurova 7, 166 29 Praha 6, Czech Republic.

² Department of Civil Engineering, Schulich School of Engineering, University of Calgary, 2500 University Drive NW, Calgary, Alberta, Canada T2N 1N4.

³ Husky Energy, 707 8th Ave. S.W., Box 6525, Station D, Calgary, Alberta, Canada T2P 3G7.

⁺ Corresponding Author: E-mail josef.zak@fsv.cvut.cz

Note: Submitted February 3, 2012; Revised December 7, 2012; Accepted December 14, 2012.

study the possibility of abridging the path from linear viscoelastic state to the nonlinear state (described here by the wheel tracking test) of a paving mix.

In this study, two methods of repetitive loading and unloading used for the testing of asphalt binders and paving mixes were investigated: the first was a compressive sinusoidal loading with small amplitude oscillations (yielding the complex modulus E^*); the second one was the wheel tracking test, where moving loads were applied through wheels with solid rubber tires, which traveled with a reciprocating motion on paving mix specimens (yielding the accumulated deformation—the rut depth). The studied paving mixes were prepared with conventional, oxidized, and polymer modified asphalt binder. The paving mixes were compacted in a Troxler Model 4140 gyratory compactor and tested in an IPC Global UTM-25 tester to determine the complex modulus. The Hamburg wheel tracking test with rubber wheels and without submersion in water was then performed on the paving mix samples at a temperature of 58°C. From the kinematics of this test, the values of the accumulated compliance function were then estimated.

The wheel tracking test generally imposes a complicated deformation field on the tested material (axial deformation is accompanied by volumetric changes and also a shear deformation, which are parts of the overall deformation). The hypothesis is tested in this research that the information from the complex modulus and the information on the rut depth can be described by a simple and flexible model of the compliance function.

Complex Modulus and the Wheel Tracking Test

Complex (dynamic) modulus, $E^*(\nu)$, of the tested samples of paving mix was determined according to AASHTO Designation TP62-07 [28]. The complex modulus is there defined by the response of the tested cylindrical sample to an axial sinusoidal - compressive stress with a small amplitude. In analogy with the shear complex modulus [19, 20], $E^* = E' + iE''$,

$$E' = \left(\frac{\sigma^0}{\varepsilon_0}\right) \cos \delta, \quad E'' = \left(\frac{\sigma^0}{\varepsilon_0}\right) \sin \delta \quad (1)$$

where σ^0 and ε^0 are amplitudes of the harmonic stress (σ) and the axial strain (ε), respectively. The phase angle, δ , is defined as the angle between the stress and the strain ($E''/E' = \tan \delta$).

In linear viscoelasticity, it is a common practice to use the components of the complex modulus for the determination of the discrete relaxation spectrum, from which the corresponding retardation spectrum is then calculated [21]. To have a good description of the linear viscoelastic properties of the tested material, one needs to know the complex modulus, E^* , over a wide frequency domain. This can be achieved via the time-temperature superposition principle [19, 20], which allows for the construction of the master curves of E' , E'' and the loss tangent, $\tan \delta$, from the values of these functions taken in a smaller frequency window at several constant temperatures. By fitting the master curves of E' and E'' to the following expressions, the relaxation spectrum, $\{e_i, \lambda_i\}$, and the retardation spectrum, $\{d_i, \Lambda_i\}$, were obtained with the help of IRIS software [22], commonly used for the characterization of polymeric systems [21, 22]:

$$E' = \sum_{i=1}^N e_i \frac{(v\lambda_i)^2}{1+(v\lambda_i)^2}, \quad E'' = \sum_{i=1}^N e_i \frac{(v\lambda_i)}{1+(v\lambda_i)^2} \quad (2)$$

The linear viscoelastic creep compliance function, $D(t)$, is calculated as (using the Voigt modes):

$$D(t) = D_g + \sum_{i=1}^{N-1} d_i \left[1 - \exp\left(-\frac{t}{\Lambda_i}\right)\right] + \frac{t}{\eta} \quad (3)$$

where η represents the viscosity and D_g is the glassy compliance.

Under the phenomenological hypothesis that a typical material element of the tested mix can be treated as a homogeneous viscoelastic material, the complex compliance, $D^* = D' - iD''$, related to the complex modulus as $D^*(\nu) = 1/E^*(\nu)$, can be obtained. The creep compliance function, $D(t)$, then should be related to the shear and the bulk compliances [19, 20]. In analogy with the known approximation for shear [19] one can test the validity of the relation $D(t) \cong |D^*| \nu_{=1/t}$.

For the wheel tracking test, one can assume that the material element in the middle of the track undergoes the same deformation as mentioned above. Then the repetitive passes over such element will produce an accumulated deformation (ε_{acc}) determined by the accumulated compliance function, D_{acc} , where $D_{acc}(t) = \varepsilon_{acc}(t)/\sigma_0$ and σ_0 is the magnitude of the applied compressive stress (636.363 kPa in the studied wheel tracking test). Thus, the situation is similar to the one of a repeated creep and recovery that is accumulated with each passing of the wheel.

It would be beneficial to know the complete time evolution of the accumulated compliance function $D_{acc}(t)$, in the wheel tracking test. Such information was not available because only the “peak” deformation (rut depth) in the n -th cycle of the loading and unloading (by a passing wheel) was recorded. Thus only the envelopes of $D_{acc}(t)$ were obtained for each of the tested samples. By combining the data of compliance function obtained from the dynamic testing (complex modulus) with the data of such an envelope (wheel tracking test), one can possibly extend the domain of information on the material (from small to larger deformations). In order to test this hypothesis, the function $D(t)$ and the envelope of D_{acc} were appended, and the composite compliance function (still denoted as $D(t)$) was studied.

Stretched Exponential Description of Creep

In previous work [18, 24, 26, 30], various conventional and polymer modified asphalt binders were studied in the repeated creep and recovery test, in shear. It was found that the classical model of the shear compliance with Voigt modes (see Eq. (3)) can be applied when the deformations were small; however, the number of modes had to be increased when the accumulated deformation or the applied shear stress was increasing. In such cases, the number of parameters of the used model of compliance function would increase to more than 20. Then it was found that the stretched exponential form of the continuous distribution of the retardation times can generate a flexible model of compliance function, and, moreover, such a model contained only five adjustable parameters [24]. Because of the flexibility of such models, it is worthwhile to investigate their capability for the description of compliance

functions discussed in this contribution. Thus, let us assume that the composite compliance functions obtained from the dynamic testing and the envelope of the accumulated compliance from the wheel tracking test can be written as

$$D(t) = D_g + D_d \left[1 - \frac{2\sqrt{at}^{1+a}}{\Gamma(1+\frac{1}{a})} K_{1+\frac{1}{a}}(2\sqrt{(at)^a}) \right] + \frac{(at)^a}{a\eta} \quad (4)$$

where $K_{1+\frac{1}{a}}$ is Macdonald's function [25] of order $(1 + 1/a)$, Γ represents the gamma function, D_d is the delayed compliance, D_g and η are the same parameters as in Eq. (3).

With the help of only five parameters, relation Eq. (4) can determine the studied compliance functions quite well, as shown in results and discussion paragraph.

In the wheel tracking test, the strains/compliance functions can be represented by their accumulated values of a representative creep and recovery test [26]. The input parameters were axial load (700 N), the speed of moving wheel (0.3 m/s), the length and the thickness of the tested sample, and the contact area (0.05×0.22 m). The nominal contact area was determined from the wheel imprint on a testing surface covered with gypsum. The size of grain of gypsum is of about 15 μm . The steel plate was sprinkled with gypsum and the load wheel was consequently placed on the plate. As already mentioned, in the wheel tracking test, the complete temporal description of accumulated tensile compliance was not known, because the data of the depth of the rut were collected only at one point of n -th cycle. In a standard test, data are collected in every 250th cycle [29]. With the progressing number of cycles (time), the tested sample of paving mix sustained deformations that gradually increased and reached the state where the damage in the material was such that the material began to flow. On the other hand, the dynamic testing probed the material on a scale of small deformations, and the material behaved as a solid.

By considering both tests together, i.e., by appending the compliance from the dynamic experiment to the envelope of accumulated tensile compliance from the wheel tracking test, one can attempt to model materials' behavior over a wide scale of deformations. Basically, the behavior of the tested sample bifurcates from linear viscoelastic behavior to nonlinear behavior. Of course, the behavior after the time of such bifurcation depends on level of the applied tensile stress [30]. Such a case was not studied here.

Materials and Testing

Five asphalt paving mixes were studied, which can be divided into two groups, according to the Superpave PG grading [27] of the asphalt binders for paving mixes. In the first group (paving mixes *A* and *B*), asphalt binders PG 70-xx were used; and, in the second group (paving mixes *C*, *D* and *E*), asphalt binders PG 64-xx were used. Paving mix *A* was prepared with oxidized asphalt binder, and paving mix *B* was prepared with asphalt binder modified with 2% (wt) of styrene-butadiene-styrene (SBS) copolymer. Paving mix *C* was prepared with straight run asphalt binder; paving mix *D*, with oxidized asphalt binder; and, paving mix *E*, with asphalt binder modified by 4% (wt) of SBS. PG grading of the used binders was based on the parameter $[|G^*|/\sin(\delta)]_{\omega=10\text{rad/s}}$, Multiple Stress, and Creep Recovery Test (MSCRT). This parameter is not well suited

for grading the polymer modified asphalts and the additional characterization by the current form of MSCRT does not change this unfortunate situation. Thus, in this contribution, the PG grading obtained "as is" was used.

All five studied paving mixes were prepared using the same paving mix design for pavement surface layers in Alberta, Canada. The mixes consisted of five mineral aggregate fractions with a maximum size of 12.5 mm. The asphalt binder content was 6.3% (wt), and no intermixtures were added. The paving mixes were designed for 6% air voids, and the density of compacted mixture was 2285 kg/m³. To obtain the dynamic moduli of the studied paving mixes, the cylindrical specimens were tested in accordance to AASHTO specification [28]. The specimens were prepared by compacting the paving mixes in the Superpave gyratory compactor (AASHTO T312-09) and reduced by coring to 100 mm in diameter. The testing frequencies were 0.1, 0.5, 1, 5, 10, and 25 Hz over the temperature range from -10°C to 80°C. When testing paving mixes, the care was taken to eliminate any data from "problematic" experiments, e.g. unstable LVDT, even slightly damaged sample due to the loading, etc. Only the data satisfying the condition that recoverable axial microstrain was in the range of 50-150 microstrains, as required by AASHTO TP62, were considered. Especially at higher temperatures, a substantial amount of data had to be omitted and the dynamic load was adjusted to comply with AASHTO TP62.

The wheel tracking tests were performed in accordance to CSN EN 12697-22+A1 [29], which is the Czech specification that is in compliance with specifications used in the European Union.

The slab (260×320×50 mm) specimen is fixed in steel mold at the constant temperature and the top surface of the specimen is taxiing by the wheel. The wheel reciprocates over the test specimen at the frequency of 26.5±1 cycles per minute. The wheel has a 20 mm-deep rubber hoop. The depth of the impression is defined as an average value of the test specimen profile on the length of 50 mm in the middle of the test specimen. The profile is measured at more than 25 points, all approximately evenly distributed. The depth of the impression of the wheel is measured in motion. The wheel tracking continues to reach 10,000 cycles or a depth of the impression of the wheel of 20 mm. This test method is commonly used for determining the resistance against permanent deformation of asphalt mixtures and material used in the EU must meet the requirements established by this methodology.

The record of the rut depth of the wheel is set to every 250th cycle. Recording of rut depth in constant sections is not commensurable to the progress of impression, especially in the initial stage of the test. The value of the rut depth in the second record point can be over 40% of the total rut depth. For these reasons, the record was set approximately and proportionally divided to progress of the impression. The specimens were not submerged in water during this test. A constant temperature was maintained (±1°C) by temperature control system thus eliminating the moisture damage. The moisture susceptibility is not discussed in this paper. The aim was to maintain similar boundary conditions in both tests.

Results and Discussion

The master curves of the dynamic material functions (E' , E'' , $\tan \delta$)

at a reference temperature of 58°C were prepared for all the tested materials in the IRIS platform [22]. A typical behavior of these functions is shown in Fig. 1 for asphalt mix sample C (conventional binder used). All the tested samples displayed similar behavior, i.e., E' increased with reduced frequency and reached its plateau at high frequencies, E'' was increasing and passing through its maximum at higher frequencies. Reduced frequency $\nu' = a_T \nu$, where a_T is the horizontal shifting factor, is very well described by the Williams-Landel-Ferry relation [19,20].

No vertical shifting was necessary to obtain the master curves of the dynamic materials functions for all the studied materials. The loss modulus, E'' , reached its absolute maximum on the displayed domain of the reduced frequencies. Similarly, the loss tangents of all the materials reached their absolute maximum well before their loss moduli did. From the behavior of dynamic material functions, it is clear that all the materials behave as linear viscoelastic solids (in the tested domain of reduced frequencies). This can be clearly seen in Fig. 1, where there is no upturn of $\tan \delta$ to the higher values for the behavior of the loss tangent at the lowest reduced frequencies (highest temperatures), usually indicating the flow of the material. Of course, it must be stressed that testing at high temperatures (greater than 80°C) was not possible due to the unreliability of data. Once the dynamic moduli were fitted to Eq. (2), IRIS can calculate the relaxation and retardation spectra, the creep compliance function, $D(t)$, and other linear viscoelastic material functions.

Note that, for all the studied materials, the approximation $D(t) \cong |D^*|_{\nu=1/t}$, can be considered. An example of this approximation for one of the studied materials is shown in Fig. 2. Thus, for paving mixes, it appears possible to use the data of master dynamic functions, E', E'' , to calculate the magnitude of the complex compliance ($D^*=1/E^*$) and transform the frequency domain to the time domain and obtain a relatively good approximation of the compliance function in the linear viscoelastic domain, i.e. without the calculation of retardation spectra. As seen from Fig. 2, the only problematic interval for such an approximation was the part of the domain that corresponded to high temperatures, where the original data also had to be considered with caution because of possible partial damage, viscoplasticity, and other nonlinear processes.

Before analyzing the wheel tracking test, several assumptions have to be put forward:

- a) The material element in the middle of the track is predominantly acted on by a compressive stress

$$\sigma(t') = \sigma_0 \sum_{n=0}^{\infty} [H(t' - nb) - H(t' - nb - a)] \quad (5)$$

where H is the unit step function and σ_0 is the magnitude of the applied stress.

The stress σ acts during the time interval of length, a , and the duration of one cycle (basically the creep and recovery) is b .

- b) The strain, $\varepsilon(t)$, is determined by the history of the compliance function D' , i.e., the following constitutive relation is assumed to hold

$$\varepsilon(t) = \int_{-\infty}^{\infty} H(t - t') D'(t - t') \frac{d\sigma(t')}{dt'} dt' \quad (6)$$

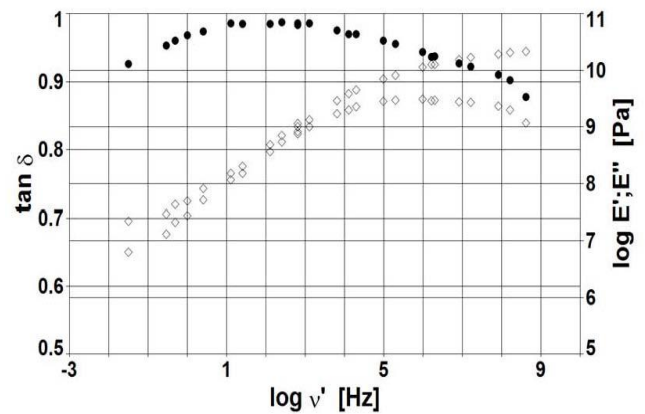


Fig. 1. Dynamic Material Functions, $T_r = 58^\circ\text{C}$, Paving Mix C. ● - $\tan \delta$, ◇ - E' and E'' .

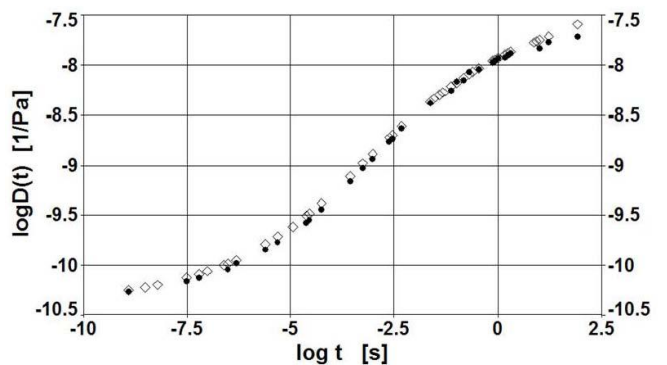


Fig. 2. Compliance Function, $T_r = 58^\circ\text{C}$, Paving Mix B. ◇ - $D(t)$ from Retardation Spectrum, ● - $D(t)$ Approximated from $|D^*|$.

Substitution of Eq. (5) into Eq. (6) then yields the accumulated deformation $\varepsilon(t)_{acc}$:

$$\varepsilon(t)_{acc} = \sigma_0 \sum_{n=0}^k \left[\frac{H(t - nb)D'(t - nb) - H(t - nb - a)D'(t - nb - a)}{H(t - nb - a)D'(t - nb - a)} \right] \quad (7)$$

The maximum accumulated deformation in k -th cycle appeared at time $t = kb + a$, where $k = 0, 1, 2, \dots$, i.e.

$$\varepsilon_{acc} = \sigma_0 \sum_{l=0}^k [H(a + bl)D'(a + bl) - H(bl)D'(bl)] \quad (8)$$

The envelope of accumulated compliance function in k -cycles is then

$$D'_{acc} = \sum_{l=1}^k [D'(a + bl) - D'(bl)] \quad (9)$$

Under the assumptions listed above, the wheel tracking test can be described when the compliance function, D' , is known. For example, data from wheel tracking test (envelope of $D'(t)$) for sample B were fitted to Eq. (9) with the form of $D'(t)$ given in Eq. (4), as shown in Fig. 3.

Combining data from the linear viscoelastic domain with available data of D'_{acc} , a composite trend of the tensile compliance (for simplicity denoted as D , in appropriate Figures) can be determined, thus covering a larger time domain and including the

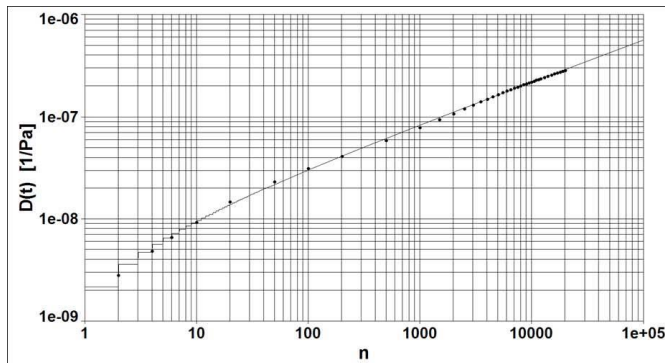


Fig. 3. Envelope of Compliance Function from Wheel Tracking Test, $T_r = 58^\circ\text{C}$, Paving Mix *B*. Fit to Eq. (9) with $D(t)$ given by Eq. (4), n - number of Cycles.

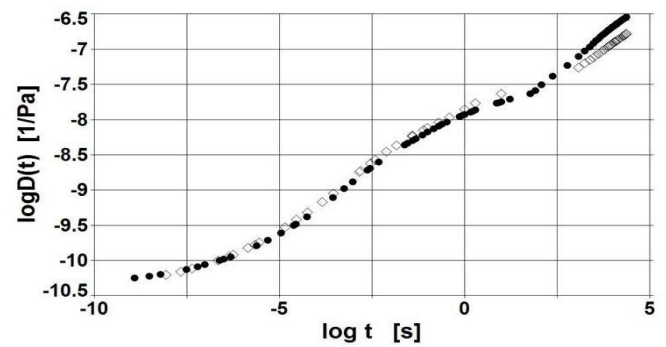


Fig. 6. Composite Compliance Function from Dynamic Data (Retardation Spectrum) and from Wheel Tracking Data (Envelope), $T_r = 58^\circ\text{C}$. ● - Paving Mix *B*, ◇ - Paving Mix *E*.

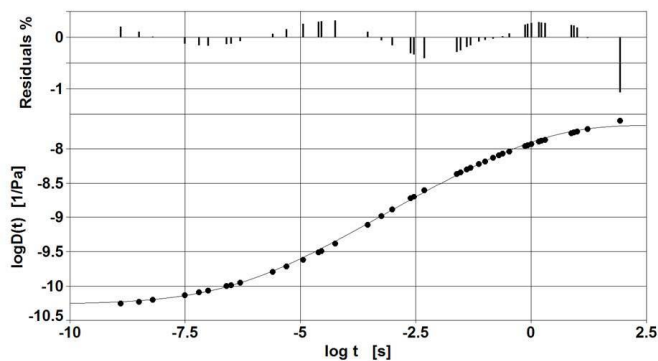


Fig. 4. Compliance Function from Retardation Spectrum, $T_r = 58^\circ\text{C}$, Paving Mix *B*. Fit to “Solid” form of Eq. (4).

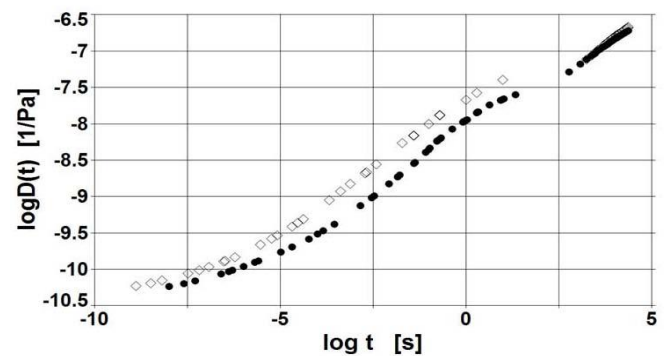


Fig. 7. Composite Compliance Function from Dynamic Data (Retardation Spectrum) and from Wheel Tracking Data (Envelope), $T_r = 58^\circ\text{C}$. ● - Paving Mix *A*, ◇ - Paving Mix *D*.

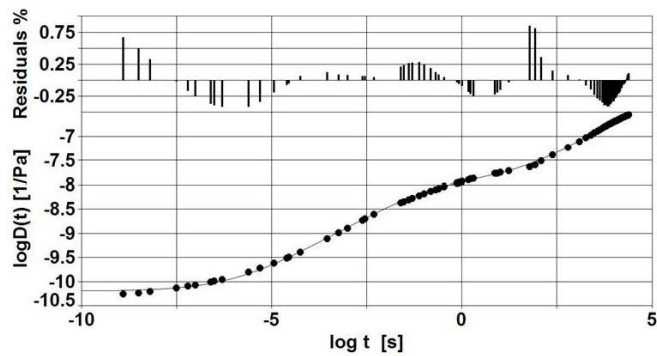


Fig. 5. Composite Compliance Function from Dynamic Data (Retardation Spectrum) and from Wheel Tracking Data (Envelope), $T_r = 58^\circ\text{C}$, Paving Mix *B*. Fit to Eq. (4).

behavior of the tested sample at deformations larger than those in the dynamic testing.

As an example, consider again sample *B*. In Fig. 4, the compliance obtained from the dynamic data is portrayed and fitted to the solid form of Eq. (8), i.e., the flow term $\frac{(\alpha t)^a}{\alpha \eta}$ was omitted. When the data from wheel tracking test were appended (envelope of $D_{acc}(t)$), the flow term had to be present in the model of $D'(t)$, i.e., the complete Eq. (4) was used. The fit of compliance to Eq. (4) is shown in Fig. 5. As seen from the portrayed residuals, the fit was very good in the whole domain of the definition, although the maximum deformation in the “dynamic” part was about 1% and the

maximum deformation in the wheel tracking test was about 20% (probably corresponding to “slightly” nonlinear behavior).

The effect of modification of the binder with SBS copolymer on the properties of the tested paving mixes is seen in Fig. 6, where the behavior of samples *B* and *E* is again portrayed by the composite compliance function, $D(t)$. The behavior of both samples was almost identical in the linear viscoelastic domain, where $D(t)$ was obtained from the dynamic data. A small difference in $D(t)$ was observed only at times obtained from the dynamic data at high temperatures ($T > 65^\circ\text{C}$).

From the data of wheel tracking test, a stronger rutting potential was identified in sample *B* (mix prepared with binder modified by 2% of SBS). Interestingly, the binder in sample *E* was characterized as PG64-XX and the binder in sample *B* as PG70-XX. Paving mix samples *A* and *D* were both prepared with oxidized binders. The binder of mix *A* was characterized as PG70-XX and that of mix *D* as PG64-XX. Fig. 7 shows that the behavior was different in the linear viscoelastic region, where the values of $D(t)$ were larger (over the whole domain of definition of $D(t)$) for mix *D*. However, the wheel tracking test “did not see” much difference between these two materials. Note that in many composite graphs of the tensile compliance function, there was a gap between the data from the dynamic experiments and the data from the wheel tracking test. The cause is that there was a difference in temperature of between 0.5°C and 1.2°C from the reference temperature of 58°C during the first

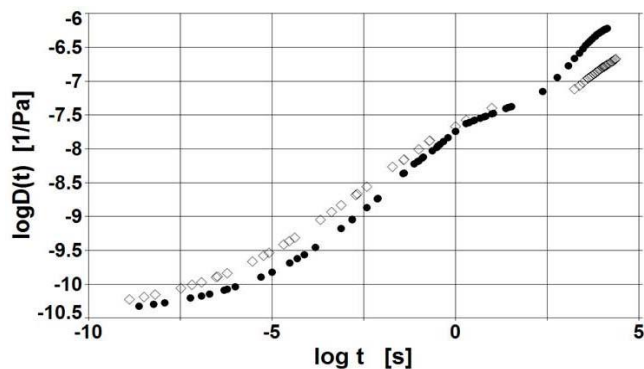


Fig. 8. Composite Compliance Function from Dynamic Data (Retardation Spectrum) and from Wheel Tracking Data (Envelope), $T_r = 58^\circ\text{C}$. ● - Paving Mix C, ◇ - Paving Mix D.

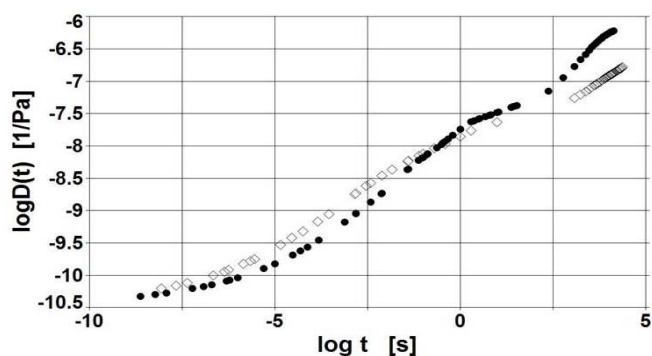


Fig. 9. Composite Compliance Function from Dynamic Data (Retardation Spectrum) and from Wheel Tracking Data (Envelope), $T_r = 58^\circ\text{C}$. ● - Paving Mix C, ◇ - Paving Mix E.

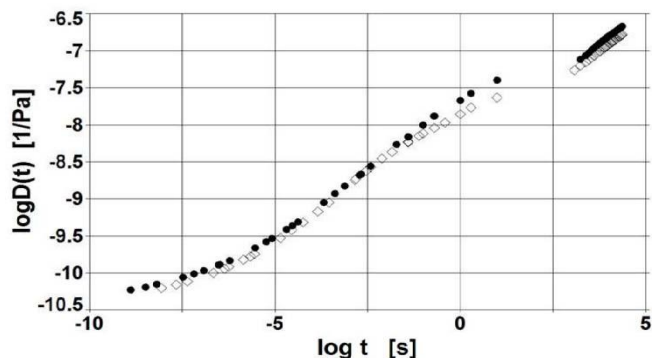


Fig. 10. Composite Compliance Function from Dynamic Data (Retardation Spectrum) and from Wheel Tracking Data (Envelope), $T_r = 58^\circ\text{C}$. ● - Paving Mix D, ◇ - Paving Mix E.

several cycles of the dynamic tests; due to such uncertainty, some data were discarded.

Comparing the mix prepared with the conventional binder (mix C) and the mix prepared with the oxidized binder (sample D), a much higher rutting potential was observed in mix C than in mix D, as shown in Fig. 8. Fig. 8 shows that the values of compliance were larger in the mix prepared with oxidized binder when the linear viscoelastic domain was portrayed; however, they were much smaller when calculated from the wheel tracking data, i.e., much higher deformations were observed in the mix prepared with

conventional binder, although the binders in both samples were characterized as PG 64-XX.

A similar observation was made for paving mixes C and E: Fig. 9 shows the comparison of the paving mix prepared with conventional binder (mix C) and the mix prepared with polymer modified binder with 4% of SBS (sample E). The shown tensile compliance function points to much smaller deformations in sample E than in mix C at the test temperature of 58°C . Both samples were characterized as PG64-XX.

Samples D and E are compared in Fig. 10. The compliances of both samples were quite similar at first; then, the values of $D(t)$ (i.e., also deformations) were smaller in the sample prepared with polymer modified binder (E). This was also true for the wheel tracking part of the portrayed tensile compliance function; however, there the values of $D(t)$ were again quite close in both samples. These two samples were characterized as PG64-XX. The observed trend of behavior of $D(t)$ started for both samples in the linear viscoelastic region and did not change during the wheel tracking test.

After observing the behavior of compliance function in several paving mixes, one can ask an obvious question: Is it possible to predict the magnitude of deformations during the wheel tracking test from the dynamic data performed at smaller deformations? As noted above, the tested paving mixes behaved as solids in the dynamic tests, i.e., the flow term in model Eq. (4) was absent. In other words, the viscosity had to be extremely large. However, the trend of the accumulated tensile compliance (appending the wheel tracking test) could be fitted to model Eq. (4) only when the tested material is capable of flow. For the composite compliance function, this means that the parameters of the model were different from the ones of the solid behavior (linear viscoelastic behavior observed in the dynamic experiments). Thus, strictly speaking, the answer to the posed question should be no; however, one can try to obtain at least a rough estimate of the deformation in the wheel tracking test from the values of the compliance function obtained from the values of the dynamic material functions E' and E'' at high frequencies. Such an estimate is shown in Fig. 11 for mix B.

Only the data of compliance $D(t)$ obtained from the data of the peak of dynamic loss modulus, E'' , were used, and model Eq. (4) was fitted to them. As seen from Fig. 11, the fitted curve was quite close to the higher values of the accumulated compliance calculated from the wheel tracking test (the residual difference was less than 10% for deformations of about 20%). Similar estimates were obtained for the rest of the tested materials. Fig. 12 shows the corresponding domain of frequencies in the dynamic experiment with the peak of E'' and the fit of this peak to the Gaussian modulus type distribution function. The fit of the glass transition peak (the range of E'' around the absolute maximum of this dynamic function) serves as an indicator of the domain of frequencies where the tested material stops flowing. The complement of this domain (the interval of frequencies on the left of this domain) then determines the flow domain on the time axis. The outlined procedure is not rigorous; however, it can serve as a method of estimation of the behavior at long times, i.e., larger deformations. For a more rigorous description of large deformation behavior, one will have to assume that the viscosity is not a parameter, but a function of time [30].

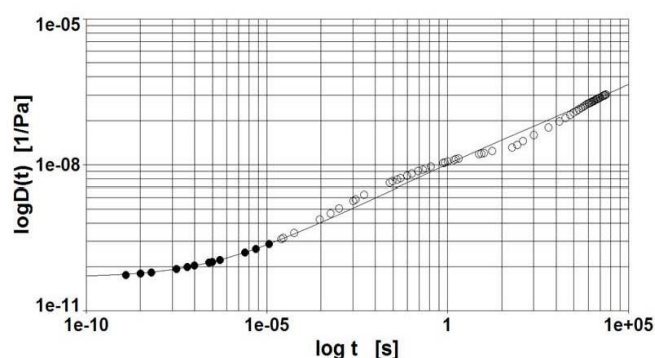


Fig. 11. Estimate of Composite Compliance Function from Peak of E'' , Paving Mix D , $T_r = 58^\circ\text{C}$. ● - Data Used for Fitting Model Eq. (4), ○ - Original Data of Composite $D(t)$.

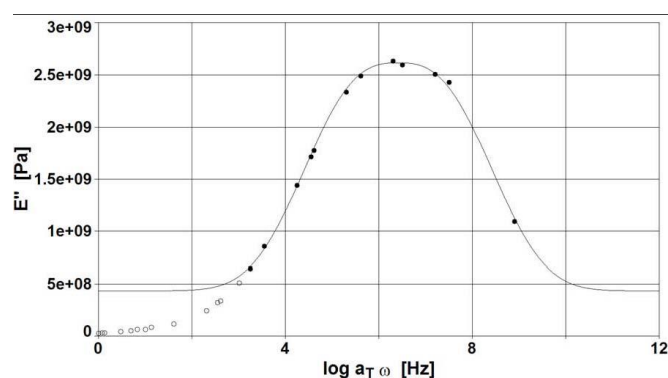


Fig. 12. Peak of Loss Modulus E'' Fitted to Gaussian Modulus Distribution, $T_r = 58^\circ\text{C}$, Paving Mix B . □ Fit, □ Data of E'' Used for Fit, ○ Data of E'' Excluded.

Conclusions

Although the linear viscoelastic properties of paving mixes seem to be unrelated to the behavior of these materials in the wheel tracking test, it was found that by transforming the complex compliance obtained from the small amplitude oscillations to the compliance function $D(t)$, a stretched time compliance model is not only able to describe the behavior of these materials in the linear viscoelastic domain, but it is also useful for the description of the behavior in wheel tracking tests.

Basically, one can say that the investigation of compliance functions can reveal more about the high-temperature behavior of paving mixes than the analysis of the dynamic material functions. This is not to say that the investigation of dynamic material functions (E' and E'') is useless. First of all, it was found that $|E^*(\omega)|$ can be used to effectively approximate the compliance function, $D(t)$, in the linear viscoelastic domain. Such compliance can then be appended to the trend of the accumulated compliance obtained from the wheel tracking test; then the composed compliance function can be fitted to the proposed (stretched time) compliance model. The advantage of the stretched time is a relatively smooth transition from the linear viscoelastic behavior to the mildly nonlinear behavior of the compliance function obtained from the wheel tracking test. Moreover, an estimate of the behavior at these higher strains can be obtained from the fitting of the

proposed compliance model to a relatively small set of data defined by the “glass transition” peak of E'' (obtained from the dynamic testing of the studied material).

The PG grading (based on the strictly linear viscoelastic domain) of the binders used for the preparation of the studied paving mixes may not reflect the behavior of mixes at larger deformations. The high-temperature behavior of paving mixes at substantially large deformations will need modification of the presented model of compliance function. In particular, the time evolution of the viscosity parameter, and the impact of high stresses have to be considered. A detailed comparison of $D(t)$ obtained from high frequencies and the values calculated from wheel tracking test is planned and it will be discussed elsewhere.

Acknowledgements

The authors would like to acknowledge Husky Energy Inc. for financial support and Mr. R. Wirth of the Department of Civil Engineering for his help in materials testing.

The article was supported by the project SGS12/040/OHK1/1T/11 of Czech Technical University in Prague.

References

- Panda, M. and Mazumdar, M. (2002). Utilization of Reclaimed Polyethylene in Bituminous Paving Mixes, *Journal of Materials in Civil Engineering*, 14(6), pp. 527-530.
- Airey, G.D. (2002). Rheological Evaluation of Ethylene Vinyl Acetate Polymer Modified Bitumens, *Construction and Building Materials*, 16, pp. 473-487.
- Airey, G.D. (2004). Styrene Butadiene Styrene Polymer Modification of Road Bitumens, *Journal of Materials Science*, 39, pp. 951-59.
- Carreau, P.J., Bousmina, M., and Bonniot, F. (2000). The Viscoelastic Properties of Polymer-modified Asphalts, *The Canadian Journal of Chemical Engineering*, 78, pp. 495-502.
- D'Angelo, J., Dongre, R., and Reinke, G. (2006). Evaluation of Repeated Creep and Recovery Test Method as an Alternative to SHRP+ Requirements for Polymer Modified Binders, *Proceedings of the Canadian Technical Asphalt Association*, pp. 143-162.
- Polacco, G., Stastna, J., Biondi, D., and Zanzotto, L. (2006). Relation between Polymer Architecture and Nonlinear Viscoelastic Behavior of Modified Asphalts, *Current Opinion in Colloid & Interface Science*, 11, pp. 230-245.
- Rowe, G., Baumgardner, G., and Sharrock, M. (2009). Functional Forms for Master Curve Analysis of Bituminous Materials, *Proceedings of the 7th International RILEM Symposium on Advanced Testing and Characterization of Bituminous Materials*, Rhodes Island, Greece, pp. 81-91.
- Wekumbura, C., Stastna, J., and Zanzotto, L. (2007). Destruction and Recovery of Internal Structure in Polymer-modified Asphalts, *Journal of Materials in Civil Engineering*, 19(3), pp. 227-232.
- Polacco, G., Kriz, P., Filippi, S., Stastna, J., Biondi, D., and Zanzotto, L. (2008). Rheological Properties of Asphalt/SBS/Clay Blends, *European Polymer Journal*, 44, pp.

- 3512-3521.
10. Sureshkumar, M.S., Filippi, S., Polacco, G., Kazatchkov, I., Stastna, J., and Zanzotto, L. (2010). Internal Structure and Linear Viscoelastic Properties of EVA/Asphalt nanocomposites, *Journal of Applied Polymer Science*, 118, pp. 557-565.
 11. You, Z., Mills-Beale, J., Foley, J.M., Roy, S., and Odegard, M. (2011). Nanoclay-modified Asphalt Materials: Preparation and Characterization, *Construction and Building Materials*, 25, pp. 1072-1078.
 12. Collop, A.C., Cebon, D., and Hardy, S.A. (1995). Viscoelastic Approach to Rutting in Flexible Pavements, *Journal of Transportation Engineering*, 121, pp. 82-92.
 13. Underwood, B.S., Yun, T., and Kim, Y.R. (2011). Experimental Investigation of the Viscoelastic Behaviors of Hot Mix-Asphalt in Compression, *Journal of Materials in Civil Engineering*, 23, pp. 459-467.
 14. Zou, G., Zhang, X., Xu, J., and Chi, F. (2010). Morphology of Asphalt Mixture Rheological Master Curves. *Journal of Materials in Civil Engineering*, 22, pp. 806-810.
 15. Van De Loo, P. (1974). Creep Test, A Simple Tool to Judge Asphalt Mix Stability, *Journal of the Association of Asphalt Paving Technologists*, 43, pp. 57-67.
 16. Ameri, G.M. (1989). Permanent Deformation Potential in Asphalt Concrete Overlays over Portland Cement Concrete Pavements. PhD Thesis, Texas A&M University, College Station, TX, USA.
 17. Hofstra, A. and Klomp, A. (1972). Permanent Deformation of Flexible Pavements under Simulated Road Traffic Conditions, *Proceedings of 3rd International Conference on the Structural Design of Asphalt Pavements*, Grosvenor House, London, England, pp. 613-621.
 18. Wasage, T.L.J., Stastna, J., and Zanzotto, L. (2010). Comparison of the Rutting Potential of Paving Mixes Produced from Different Asphalt Binders with the Same Superpave High-temperature Performance. *Canadian Journal of Civil Engineering*, 37, pp. 1406-1413.
 19. Ferry, J.D. (1980). *Viscoelastic Properties of Polymers*, John Wiley, New York, USA.
 20. Tschoegl, N.W. (1989). *The Theory of Linear Viscoelastic Behavior*, Springer, Berlin, Germany.
 21. Baumgartel, M. and Winter, H. (1989). Determination of the Discrete Relaxation and Retardation Time Spectra from Dynamic Mechanical Data, *Rheologica Acta*, 28, pp. 511-519.
 22. *IRIS Development LLC*. (2008). 14 Elm Street, Amherst, MA 01002-2007, USA.
 23. Gross, B. (1953). *Mathematical Structure of the Theories of Viscoelasticity*. Herman, Paris, France.
 24. Polacco, G. and Stastna J. (2008). Accumulated Strain in Polymer-modified Asphalts. *Rheologica Acta*, 47, pp. 491-498.
 25. Gradshteyn, L.S. and Ryzhik, L.M. (1980). *Tables of Integrals, Series and Products*, Academic, New York, USA.
 26. Wasage, T.L.J., Stastna, J., and Zanzotto, L. (2010). Repeated Loading and Unloading Tests of Asphalt Binders and Mixes, *Road Materials and Pavement Design*, 11, pp. 725-744.
 27. *AASHTO Designation: M320-9. Precision Estimates for AASHTO Test Method T308 and the Test Methods for Performance-Graded Asphalt Binder in AASHTO Specification M320*, (2005).
 28. *AASHTO Designation: TP 62-07. Standard Method of Test for Determining Dynamic Modulus of Hot-Mix Asphalt Concrete Mixtures*, (2007).
 29. *CSN EN 12697-22+A1. Bituminous Mixtures Test Methods for Hot Mix Asphalt – Part 22: Wheel Tracking Test*, (2008).
 30. Wasage, T.L.J., Stastna, J., and Zanzotto, L. (2011). Rheological Analysis of Multi-stress Creep Recovery (MSCR) Test, *International Journal of Pavement Engineering*, 12, pp. 561-568.